Engineering and Technology Journal
Journal homepage: https://etj.uotechnology.edu.iq

Enhancing the surface integrity of gas turbine compressor blades using alumina abrasives in magnetic finishing: an experimental approach

Tahseen M. Salman*, Saad K. Shather, Baraa M. H. Albaghdadi

College of Production Engineering and Metallurgy, University of Technology-Iraq, Alsina'a street, 10066 Baghdad, Iraq.
*Corresponding author Email: pme.19.02@grad.uotechnology.edu.iq

HIGHLIGHTS

- Magnetic Abrasive Finishing was applied to restore gas turbine blades with fatigue and surface damage.
- Surface finishing with Al_2O_3 abrasives reduced roughness by 33.7%, improving fatigue crack resistance.
- Optimal finishing was achieved at 630 rpm, 1.8 mm gap, and 30% abrasive ratio.
- Maximum material removal occurred at 400 rpm, 1.8 mm gap, and 40% abrasive concentration.
- The study showed MAF as a scalable solution for turbine blade reconditioning despite noted limitations.

Keywords:
MAF
Fatigue failure
Al_2O_3 powder
turbine blades
surface finishing
SR improvement

ABSTRACT

Magnetic Abrasive Finishing (MAF) is a highly effective technique for enhancing the surface integrity of high-value components with complex geometries, owing to its non-contact, flexible, and precisely controllable nature. This study investigates the use of Al_2O_3 (alumina) powder as an abrasive medium in the MAF process, selected for its high hardness, thermal stability, and chemical inertness. Although Al_2O_3 is only weakly paramagnetic, it was successfully incorporated into the magnetic abrasive brush through mechanical blending with ferromagnetic particles that respond to the magnetic field. This hybrid abrasive system enables effective control of finishing forces, leading to significant improvements in surface quality and the elimination of surface defects. A series of controlled experiments was conducted to evaluate the influence of key process parameters—rotational speed, working gap, abrasive mixing ratio, and processing time—on surface roughness and material removal. The results demonstrated that the inclusion of Al_2O_3 in the MAF process significantly enhanced surface finish and micro-crack removal without compromising dimensional accuracy. Optimal finishing performance was achieved at a rotational speed of 630 rpm, a gap of 1.8 mm, and a mixing ratio of 30%, resulting in a maximum surface roughness improvement of 33.7%. Furthermore, the elimination of micro-cracks contributed to a substantial increase in fatigue resistance. While most trials yielded consistent results, one test showed slightly lower performance due to an increased working gap, reduced brush flexibility, and potential contamination from dense Al_2O_3 particles. The study suggests that Al_2O_3-enhanced MAF is a promising method for extending the service life of metal components.

1. Introduction

The compressor blades in a gas turbine are vital as they significantly influence the engine's performance and efficiency. Their primary role is to compress substantial volumes of air into a reduced space, so markedly elevating the air pressure before it enters the combustion chamber [1]. The elevated air pressure facilitates improved combustion, leading to enhanced power production. Turbine blades endure severe operational conditions, encompassing significant heat variations, intense vibrations, and considerable centrifugal forces. The amalgamation of these stresses frequently precipitates the formation of micro-cracks, which, if neglected, may extend deeply into the blade structure, ultimately culminating in blade fracture [2-4]. A cracked turbine blade may become dislodged and ejected within the compressor, resulting in significant damage to neighboring blades. Cascading failures may result in the total failure of the compressor system in gas turbines. This situation underscores the essential requirement for prompt treatment and surface conditioning of turbine blades, including the elimination or alleviation of surface cracks, to avert catastrophic failure. An actual instance of this transpired in the third unit of the Al-Quds Thermal Power Station, when blade failure resulted in significant damage to the compressor section. The exorbitant expense of turbine blades—frequently reaching thousands of dollars each—has necessitated their prompt refurbishment. Often, these blades undergo

http://doi.org/10.30684/etj.2025.161592.1970
Received 16 June 2025; Received in revised form 03 August 2025; Accepted 16 August 2025; Available online 22 October 2025
2412-0758/University of Technology-Iraq, Baghdad, Iraq

reconditioning via surface finishing techniques conducted in adjacent nations like Iran, where refurbishing generally costs around fifty percent of the cost of producing new blades. This study seeks to assess the viability of locally repairing turbine blades to prolong their operational lifespan and diminish reliance on foreign sources, thus enhancing cost-effectiveness and self-sufficiency in blade maintenance and production. Various finishing techniques are employed to attain superior surface quality on gas turbine blades, including Magnetic Abrasive Finishing (MAF), Abrasive Flow Machining (AFM), electropolishing, superfinishing, and shot peening [5-7]. Magnetic abrasive finishing (MAF) is regarded as the superior method for turbine blade surfaces with complex geometric shapes. MAF achieves a superior surface finish by employing a magnetic field to regulate small abrasive particles, facilitating accurate and delicate material removal without compromising the blade's aerodynamic profile [8-11]. It generates exceptionally clean, reflective surfaces while preserving the intricate geometry of the blades. Furthermore, MAF does not induce mechanical strains or surface fractures, which is essential for the longevity and efficacy of the blades. The removal of fatigue crack layers is a vital application of MAF, as these layers undermine the structural integrity of components subjected to cyclic pressures [12]. Magnetic abrasives, drawn to the surface, function as a flexible brush that polishes and smooths the material without inflicting damage. [13,14]. This study investigates the incorporation of Al_2O_3 abrasive material into the MAF to enhance its performance. While Al_2O_3 is a paramagnetic material with weak magnetic responsiveness, its selection for MAF is based on its exceptional mechanical properties, including high hardness, thermal stability, and chemical inertness, which make it highly effective in surface finishing applications. In the MAF process, the magnetic field primarily serves to control the overall abrasive brush formed by the ferromagnetic particles (such as iron or carbonyl iron powder). These ferromagnetic particles are magnetically responsive and form the primary structure of the brush under the influence of the external magnetic field. The role of Al_2O_3, in this case, is as a non-magnetic abrasive additive, which becomes mechanically entrapped or distributed within the ferromagnetic matrix.

Zhou et al. [15], proposed integrating ultrasonic vibration with magnetic abrasive finishing (MAF) to enhance efficiency and surface integrity in finishing titanium parts. The results showed ultrasonic MAF facilitates micro-removal of surface material and reduces or eliminates deterioration of surface lattice structure caused by milling forces. Khangura et al. [16], studied the potential of Magnetic Abrasive Finishing (MAF) in removing the recast layers formed on cylindrical specimens (EN 31 steel) machined by Electrical Discharge Machining (EDM). Experimental results show up to an 80% improvement in surface finish with no evidence of micro-cracks, voids, or recast layers on the finished surfaces. Zhang et al. [17], investigated magnetic abrasive finishing (MAF) of selective-laser-melted 316L stainless steel. The results showed the MAF method effectively removed most partially bonded particles and balling defects. Arora and Singh [18], introduced a theoretical model to predict material removal volume and surface roughness reduction in the straight bevel (SB) new magnetorheological (MR) bevel gear finishing (BGF) method for gears. Surface roughness decreases from 450–90 nm after 90 minutes of MR finishing, improving surface morphology and eliminating initial grinding marks and cracks. Ahmad et al. [19], explored the application of Magnetic Abrasive Finishing (MAF) for achieving defect-free micro/nano surface finishes, particularly focusing on challenging materials like Ti-6Al-4V alloy. Wang et al. [20], used the fluid magnetic abrasives (FMA) polishing technique to improve the micro-shaft surface quality produced by the wire electrical discharge grinding (WEDG) process, removing recast layers, discharge craters, and micro-cracks. Results indicate significant surface roughness reduction and removal of recast layers, enhancing surface quality without micro-shaft deformation. Li et al. [21], agreed with Yan Wang and showed the same result. Rasouli and Nori [22], investigated the process parameters of Magnetic Abrasive Finishing (MAF) for refining the free surfaces of titanium blades. Results reveal that employing the magnetic abrasive method can reduce blade surface roughness by up to 33%.

This study aims to improve surface quality and eradicate microscopic fractures that, if neglected, may proliferate under cyclic load and result in premature failure, especially in high-value, geometrically intricate components. By swiftly rectifying these surface imperfections, the aim is to prolong the operating longevity of these components and facilitate efficient restoration before catastrophic breakdown. The study centers on the compressor blade of a GE gas turbine, chosen as the test specimen due to its substantial production expense and complex geometry. This study utilizes Al_2O_3 (aluminum oxide) powder as the abrasive medium in the Magnetic Abrasive Finishing (MAF) method to attain enhanced surface finishing and defect elimination.

2. Mechanism of MAF processes

Magnetic Abrasives Finishing (MAF) utilizes the manipulation of Magnetic Abrasive Particles (MAPs) within a magnetic field to enhance the surface of a workpiece. A magnetic field is first created between two poles, with the workpiece situated within this field [23-26]. Figure 1 illustrates the MAF process with weakly attached magnetic abrasive material. Magnetic abrasive particles (MAPs), consisting of abrasive and magnetic substances, occupy the voids between the workpiece and the magnet. Upon activation of the magnetic field, it aligns the MAPs along its lines of force, configuring them into a flexible brush-like formation [27-28]. The magnetic brush is systematically moved across the surface of the workpiece, delicately abrading and smoothing it by eliminating material [29-31]. Classification of Magnetic Abrasive Finishing (MAF) based on workpiece geometry includes external finishing for cylindrical shafts or flat plates and internal finishing. MAF is engineered to complete interior bores, tubes, and intricate internal geometries as illustrated in Figures (2 and 3). This study introduces a novel method designed to eliminate tiny cracks caused by fatigue in critical turbine blade materials, thereby meeting the industry's demand for longer-lasting components. This study differs from earlier research, which primarily focuses on using magnetic abrasive finishing (MAF) for polishing surfaces or removing recast layers. Instead, it specifically targets the removal of layers of fatigue cracks in turbine parts that experience repeated stress, a topic that has received little prior study. A special MAF system was created that uses a coil made of 5200 loops of 0.6 mm copper wire and a specific mix of abrasive Al_2O_3 to get rid of microcracks without damaging the material. Additionally, the study offers a comprehensive understanding of how key parameters—such as abrasive

type, rotational speed, gap distance, and abrasive mixing ratio—affect crack removal efficiency. While some larger cracks persist, the controlled removal of microcracks has proven critical for enhancing component durability under fatigue conditions.

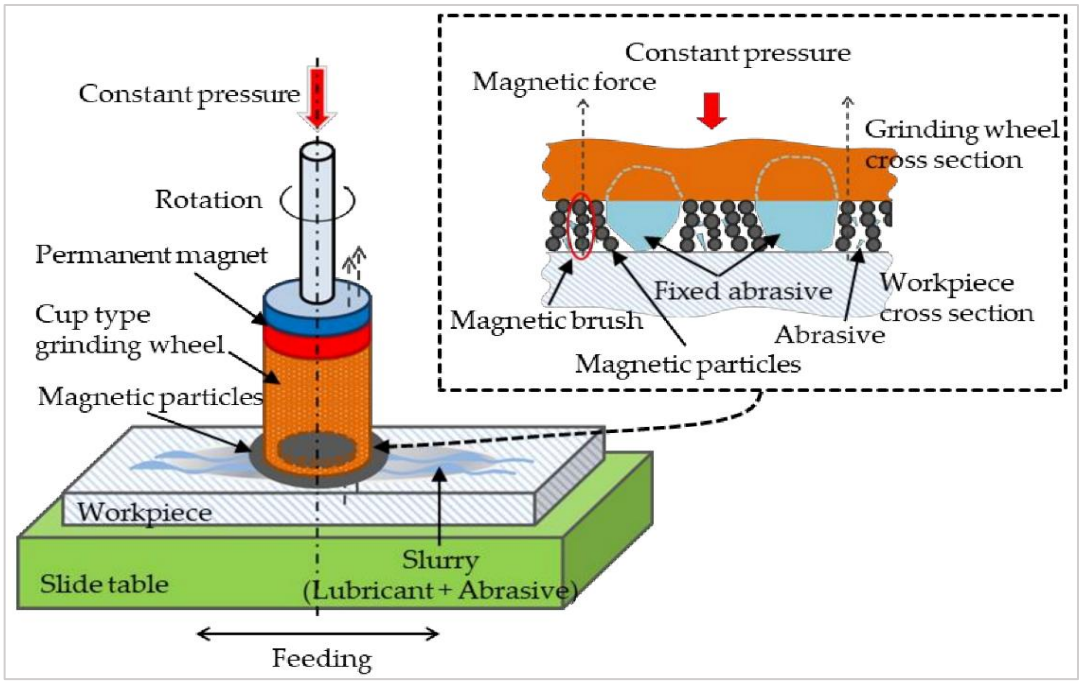

Figure 1: Schematic diagram of the MAF process with loosely bonded magnetic abrasive media [32]

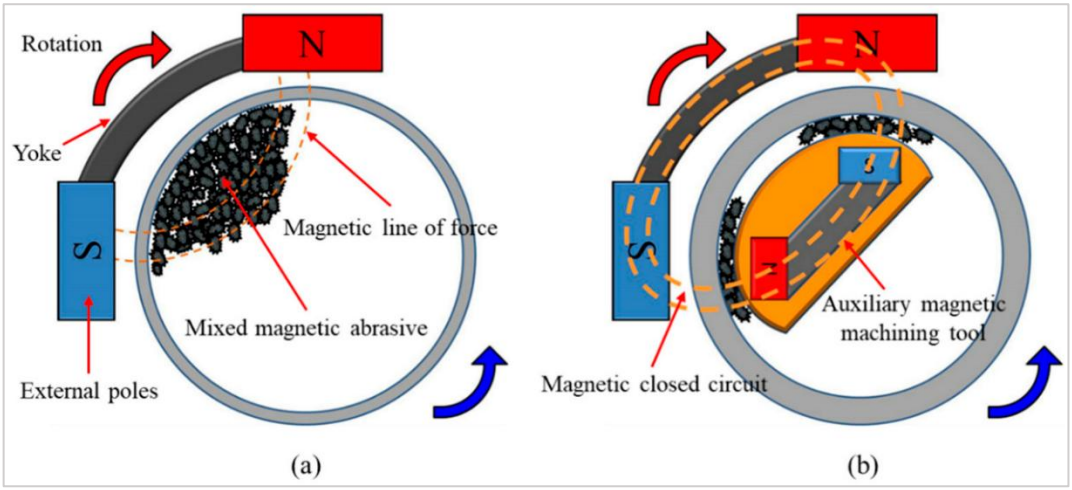

Figure 2: Schematic of MAF processes: a) MAF for inner tubes b) MAF with auxiliary magnetic machining tool [33]

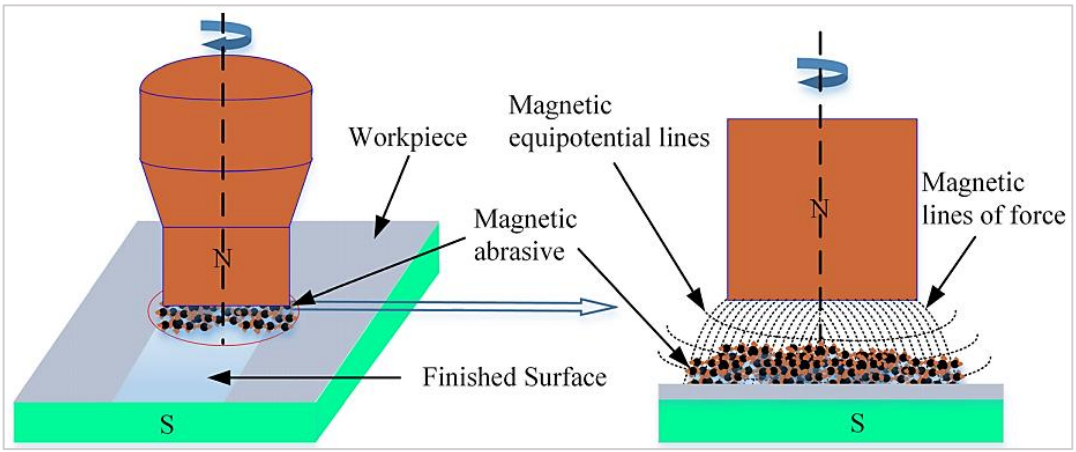

Figure 3: Mechanism of MAF for flat surface [34]

3. Methodology

3.1 Experiment setups

This study evaluates the effectiveness of Al_2O_3 as an abrasive powder in magnetic abrasive finishing (MAF) to remove fatigue crack layers from metallic surfaces. The setup uses Taguchi to simulate controlled finishing conditions, allowing analysis of interactions between abrasive particles and fatigue crack layers. The study uses fractional factorials for comprehensive research. Table 1 presents nine experiments designed by Taguchi, which have three input parameters and three levels as shown. Table 2 delineates the fixed parameters of the process conditions.

Table 1: The parameters change of the MAF process and Taguchi designs levels

Input parameter	Levels			Unit
	Level 1	Level 2	Level 3	
Tool rotation speed	400	630	800	r.p.m
Gab distance	1.3	1.8	2.3	mm
Abrasive mixing ratio	30	40	50	%

Table 2: The constant parameters process condition

Parameters	Discerption	Unit
Voltage supply	48 v	volt
Coil properties	Pure Copper (5200), no. of turns, (0.6) mm is the diameter of the coil	Number of coils
Finishing Time	10 min	minutes
Workpiece type	AISI 403 stainless steel	
Tool type	Stainless steel	
Workpiece dimension	(30×10×5) mm flat surface	mm
Abrasive grain size	300	um
Machining	A drilling machine (Taksan model) was used.	

The drilling machine used in this work is the Taksan Company Model BR 40/2x1250 Radial Drilling Machine, as shown in Figure 4. Surface topology was examined using a light microscope. Observations were conducted to elucidate the surface topography and minute fissures over the maximum feasible region.

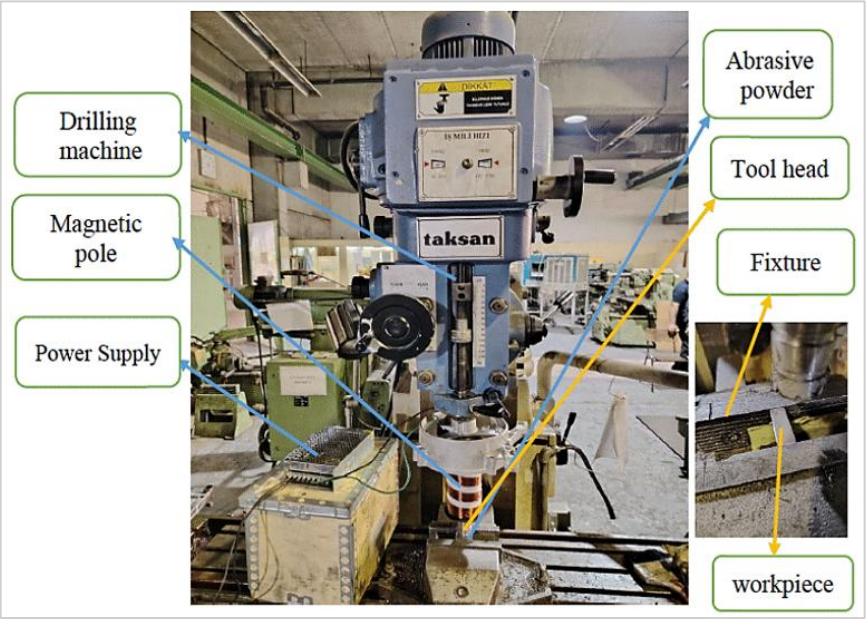

Figure 4: The drilling machine

3.2 Tool preparation (coil, pole)

The initial step in preparing a coil on a solid shaft for the Magnetic Abrasive Finishing (MAF) process involves the selection of raw materials, specifically a ferromagnetic solid shaft (either stainless steel or copper) and insulated copper wire with appropriate gauge and thermal resistance. The shaft is cleaned utilizing a Turing machine of type (WEISSER HEILBRONN HEKTOR in the Diyala General Company, Iraq - Diyala, with the entire dimension employed for the installation of other critical components, including slip rings and plastic rolls. A plastic insulating roll is employed to separate the electrical connection between the lip and the coil. The slip rings facilitate the transfer of electrical power from the stationary wire to the rotating shaft. All the parts were assembled to produce the MAF coil illustrated in Figure 5.

Figure 5: Installing parts on the solid shaft and its position

3.3 Workpiece preparation

A compressor blade for a gas turbine was selected to ensure the turbine's efficient and dependable performance. The compressor blade is considered a vital and expendable element in gas turbines because of its complex geometric configuration, high production costs, the particular alloy employed, and its durability against corrosion, thermal stress, and cyclic loading. Furthermore, the prevalence of manufacturing firms in the reconditioning process requires an analysis of the blade's design and the development of suitable strategies to extend its longevity. Figure 6 illustrates the compressor blades utilized in frame nine from General Electric. Figure 7 displays SEM fractography images analyzed to assess surface morphology and presents two images taken from different regions of the turbine blade—specifically, the tip and the base of the blade. These images illustrate zones of damage and areas of stress concentration associated with the presence of micro-cracks. The purpose of these observations is to validate and document the existence of surface defects, such as micro-cracks and concavities, which are indicative of stress concentration zones. This serves as a preparatory step for the experimental study. The images confirm that both the upper and lower regions of the blade were subjected to mechanical stresses and developed micro-cracks that significantly affected the blade's structural integrity. The SEM results supported the experimental findings by illustrating the extent and type of surface damage that occurred under various machining conditions for turbine blades.

Figure 6: Compressor blades of frame 9 from the GE company

Due to the difficulty in obtaining a compressor blade, one blade was procured and divided into nine samples, each measuring 30 × 10 mm. Table 3 below presents the chemical composition of AISI 403 stainless steel, utilized in the manufacture of compressor blades and turbines.

Table 3: Chemical composition of AISI 403 stainless steel [35]

Element	C	Si	Mn	Cr	Ni	P	S	Fe
AISI 403	0.15	0.50	1.0	11.5-13	…	0.04	0.03	Balance

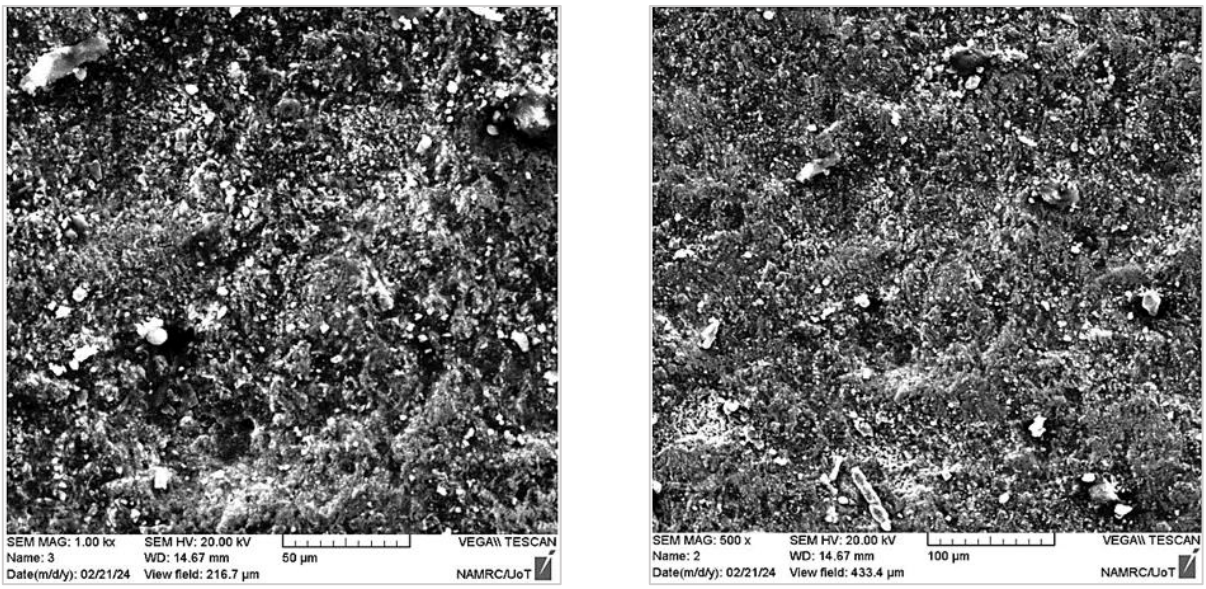

(a) **(b)**

Figure 7: (a and b) SEM fractography that illustrates surface morphology and failure characteristics, including crack initiation sites and surface irregularities before machining using the MAF process

3.4 Powder preparation

The formulation of abrasive powders is essential for the efficacy of the magnetic abrasive finishing (MAF) process. The preparation process commences with the calculation of the grain size of the abrasive and iron granules before mixing, followed by the measurement of their weight using a precise scale according to the required mixing ratio. Three alumina mixing ratios—30, 40, and 50% were prepared by blending the specified proportions into a total mixture weight of 10 grams. The components were thoroughly mixed to ensure uniform distribution. The mixture is thoroughly combined, and the binding agent resin, K-MASTICE/MASTIC FOR MARMI, is incorporated. The mixture is thoroughly combined and baked in the oven for one hour at a temperature of 250-300 °C. It remains for an entire day. Subsequently, it is extracted and pulverized to achieve the desired granule size. Figure 8 illustrates the Al_2O_3 abrasive before and after its amalgamation with iron. The grain size of alumina powder was determined by sieve analysis following ASTM E11-17. We weighed a dried sample and mechanically shook it through a series of standardized sieves with decreasing mesh sizes for 10–15 minutes. The mass retained on each sieve was measured, and the test was repeated three times for accuracy. The grain size distribution was calculated based on the cumulative weight percentages, providing a reliable average grain size for the powder. The subsequent details pertain to the materials and the experimental configuration:

1) Electrolytic iron powder, 300 mesh, 98% purity, R:11, S:16-33. CAS Number: 7439-89-6.
2) Standard liquid resin characteristics (25 °C): refer to Table 4.
3) Highly pure aluminum oxide (specially fused alumina), including a minimum of 99.5% AL_2O_3.
4) Lastly, incorporate one drop of methyl ethyl ketone peroxide, CAS No: 1338-23-4.

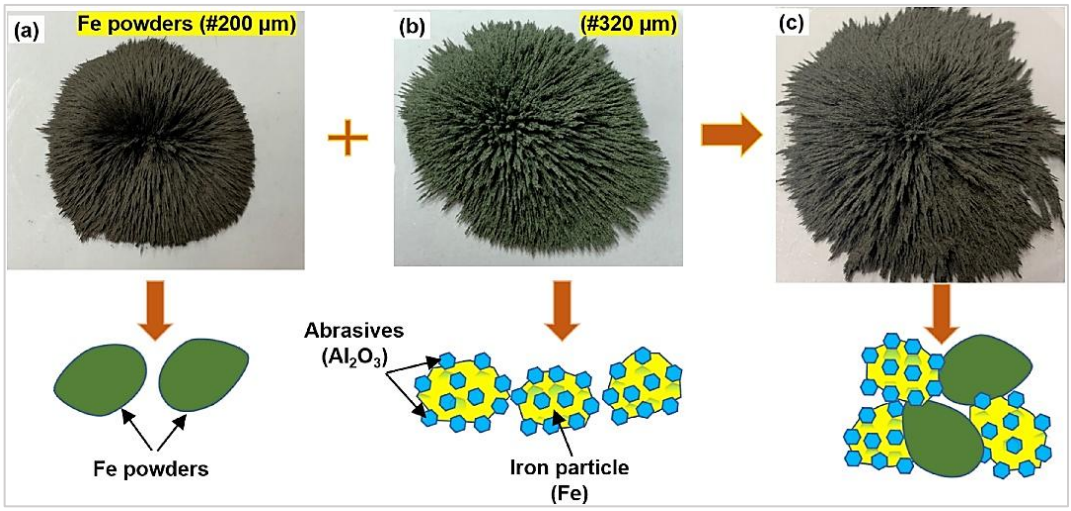

Figure 8: Preparation of magnetic abrasive tools: a) Fe powder (Fe#200), b) Al_2O_3/iron-based composite abrasives, and (c) mixture of magnetic abrasive tools [36]

Table 4: Resin properties

Percent solids	61-70%
Viscosity – Brookfield, cps spindle 3@60 rpm	450-700 cps
Appearance	Clear, yellowish
Acid value	18-24
Specific Gravity	1.04 ± 0.02
Pounds per Gallon	9.2
Flash Point Range, °C	33

4. Results and discussion

Employing Taguchi design, we acquire 9 samples as demonstrated in Table 5. Three measurements of surface roughness (SR) were acquired, and their mean was computed. The percentage increase of %SR was determined using Equation (1). The material removal rate (MRR) for each specimen was determined using Equation (2). Time is constant; therefore, we omit it from the MRR equation.

$$SR\% = \frac{SR\ after - SR\ before}{SR\ before} \times 100\% \quad (1)$$

$$MRR = (W2 - W1)/\ T \quad (2)$$

when: MRR=Material removal rate, W_2=weight before MAF process, W_1=weight after MAF process, T=time of the process, SR%=Surface improvement ratio, SR after=after MAF process, SR before=before MAF process.

Table 5: Taguchi design for the 3 different parameters and output response

NO. Of specimen	Speed (r.p.m)	Gab Distance (mm)	Mixed Abrasive ratio (%)	SR (µm) before process	SR (µm) after process	SR μm improvement(%)	MRR (g)
1	400	1.3	50	0.7	0.73	0.476	0.0035
2	400	1.8	40	0.96	0.772	19.583	0.0195
3	400	2.3	30	0.841	0.79	6.024	0.0042
4	630	1.3	40	0.716	0.6	15.363	0.0065
5	630	1.8	30	0.802	0.567	33.70	0.0028
6	630	2.3	50	0.69	0.63	10.09	0.0032
7	800	1.3	30	0.598	0.59	0.445	0.0038
8	800	1.8	50	0.67	0.595	11.19	0.0041
9	800	2.3	40	0.75	0.68	9.15	0.0088

4.1 Surface roughness (SR)

The study reveals that rotational speed, gap distance, and mixing ratio significantly impact surface roughness, as shown in Figure 9. The results indicate a substantial effect of rotational speed, with the minimum recorded at 400 rpm, signifying inferior surface quality. The surface roughness is significantly enhanced at 630 rpm, indicating optimal conditions, but experiences a slight decline at 800 rpm. The gap distance demonstrates a moderate impact, with 1.3 mm resulting in average performance, 1.8 mm achieving optimal surface quality, and 2.3 mm leading to deterioration. The mixing ratio exhibits a non-linear trend, with a 50% ratio yielding moderate surface quality, a 40% ratio resulting in inferior outcomes, and a 30% ratio markedly enhancing surface roughness. The ideal parameters correspond to a 30% mixing ratio. Departing from these standards diminishes surface quality. Table 6 presents the analysis of variance for SR.

Table 6: Analysis of variance for SR

Source	DF	Adj SS	Adj MS	F-Value	P-Value
Regression	3	0.038542	0.012847	2.48	0.176
Rotation Speed	1	0.034167	0.034167	6.60	0.050
Gap	1	0.004231	0.004231	0.82	0.407
Mixing ratio	1	0.000143	0.000143	0.03	0.874
Error	5	0.025867	0.005173		
Total	8	0.064409			

The majority of studies enhanced %ΔSR, with the optimal SR recorded at 33.7 µm and the minimal SR improvement at 0.476 µm. Meant the minus symbol, which denotes diminished improvement in surface roughness, to signify a decrease in the process's efficiency. External variables impacting the process, particularly surface pollution, may also be responsible for the decline in performance. The study mentions that broken Al_2O_3 particles can get into and stick to surfaces. Still, it doesn't explain how these particles break under pressure, how they wear down over time, or how different metals react—especially if softer metals like aluminum are more affected than harder ones like steel. The study does not provide numbers on how much contamination there is and how it affects mechanical performance, and it suggests possible solutions like stronger Al_2O_3 types,

protective coatings, or better cleaning methods. The ANOVA analysis reveals that rotation speed exerts the most substantial influence on surface roughness, followed by gap distance and then abrasive mixing ratio. Thus, optimizing the rotational velocity can more effectively aid in diminishing surface roughness. The normal probability plot depicted in Figure 10 indicates that the residuals closely conform to the red reference line, implying they are almost normally distributed. This outcome corroborates the hypothesis of normality in the ANOVA and the regression equation, as shown below in Equation 3:

$$SR = 0.772 - 0.000376\ \text{Rotation Speed} + 0.0531\ \text{Gap} + 0.00049\ \text{MixingRatio} \quad (3)$$

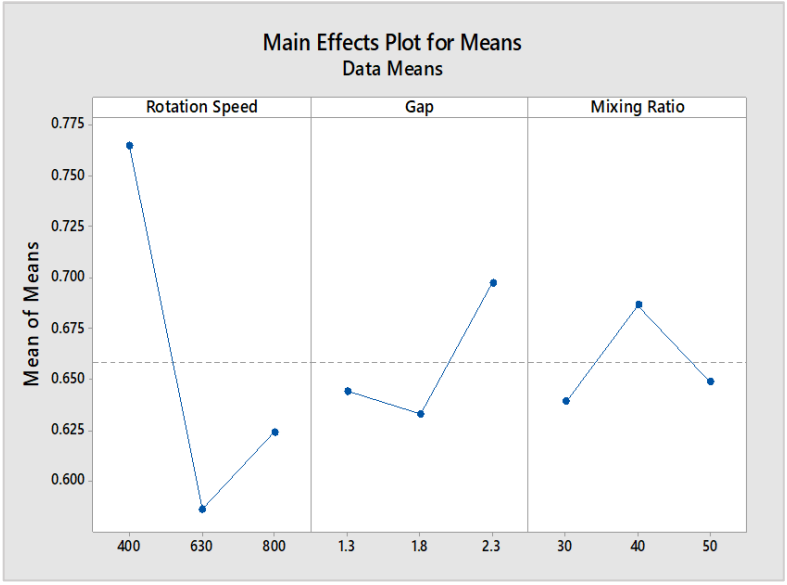

Figure 9: Main Effects plot for surface roughness (SR)

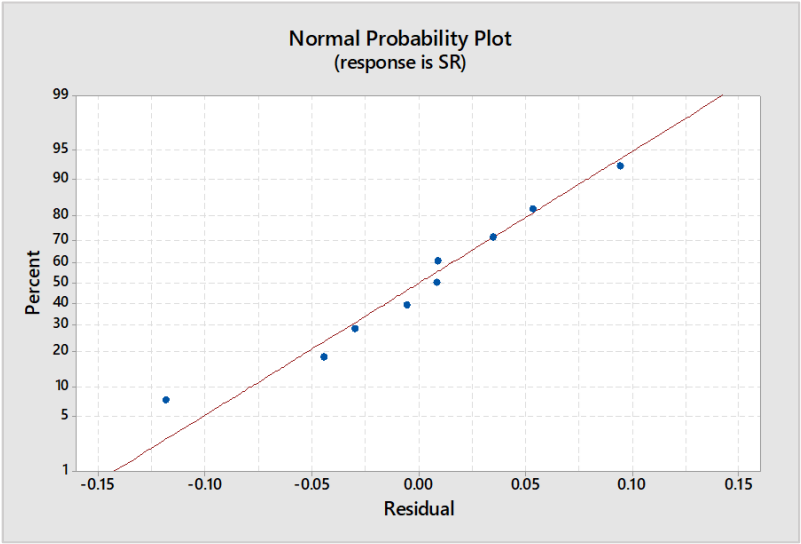

Figure 10: The normal probability plot for (SR)

The significant decline in performance at spindle speeds beyond 400 rpm may be ascribed to the instability of the magnetic abrasive brush at elevated rotational velocities. At 630 rpm, centrifugal forces may diminish the brush's contact with the surface, thereby impairing the efficacy of crack removal and surface finishing. This illustrates the importance of controlling spindle speed to achieve a balance between material removal and brush stability.

4.2 Material removal rate (MRR)

Figure 11 illustrates the impact of rotational speed, gap distance, and mixing ratio on the material removal rate (MRR), serving as the primary effects figure for means. The results indicate a substantial effect of rotational speed, with the lowest signal-to-noise ratio recorded at 400 rpm, signifying inferior surface quality. The signal-to-noise ratio significantly enhances at 630 rpm, indicating optimal surface roughness, but experiences a slight decline at 800 rpm. The gap distance demonstrates a moderate influence, with 1.3 mm resulting in average performance, 1.8 mm producing optimal surface quality, and 2.3 mm leading to deterioration. The mixing ratio exhibits a non-linear trend: a 50% ratio yields moderate surface quality, 60% results in inferior outcomes, and 70% markedly enhances surface roughness. The ideal parameters for attaining optimal surface roughness are 630

rpm for speed, 1.8 mm for gap distance, and a 70% mixing ratio. Departing from these levels diminishes surface quality. The variance analysis for MRR is shown in Table 7.

Table 7: Analysis of variance for MRR

Source	DF			Adj SS	Adj MS	F-Value	P-Value
Regression	3			0.000202	0.000067	15.00	0.003
Rotation Speed	1			0.000003	0.000003	0.62	0.462
Gap	1			0.000002	0.000002	0.43	0.538
Mixing ratio	1			0.000001	0.0000004	0.09	0.769
Error	6	0.000027	0.000004				
Total	9	0.000229					

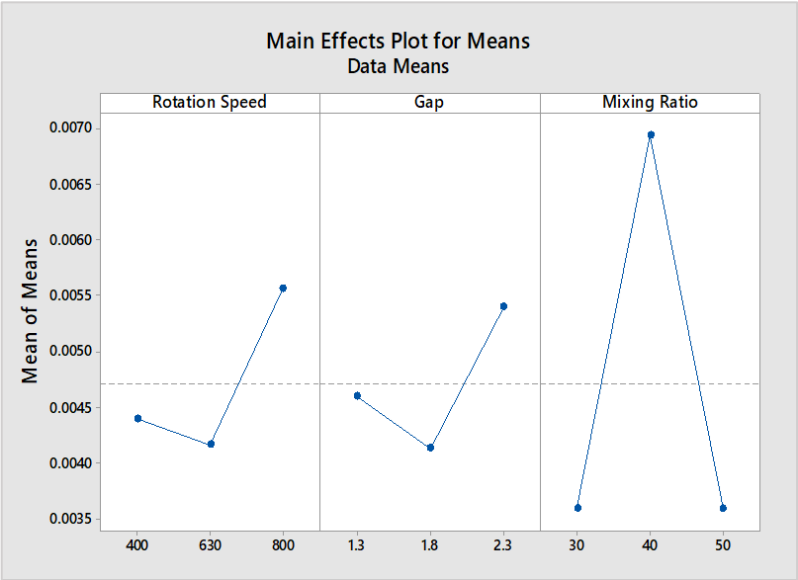

Figure 11: Main effects plot for material removal rate (MRR)

The normal probability plot for MRR shown in Figure 12 demonstrates that the residuals closely align with the red reference line, suggesting that they are approximately normally distributed. This result validates the assumption of normality in the ANOVA and the Regression Equation as shown below in Equation 4.

$$MRR = 0.000003\ \text{Rotation Speed} + 0.00100\ \text{Gap} + 0.000017\ \text{Mixing Ratio} \quad (4)$$

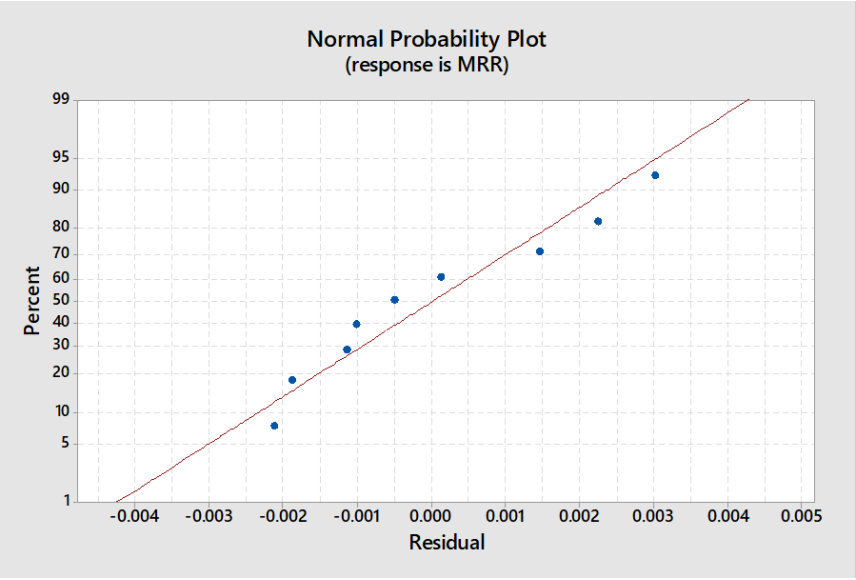

Figure 12: The normal probability plot for the (MRR)

4.3 Surface topology

Magnetic Abrasive Finishing (MAF) markedly enhances surface topology. The surfaces exhibit microcracks resulting from applied cyclic stresses, which adversely impact functional performance. Following MAF, the abrasive engagement of magnetic

particles and abrasives enhances the surface, reducing peaks and leveling valleys to achieve a uniform and polished finish, thereby significantly lowering roughness values. Observation of the samples before and after the Magnetic Abrasive Finishing (MAF) procedure demonstrated that the MAF treatment efficiently eliminated the fine fractures generated during the workpiece's use. Nonetheless, certain samples demonstrated no notable enhancement, which can be ascribed to discrepancies in the selection of process parameters. The data demonstrate that the MAF technique effectively removed certain fine fractures, whereas bigger cracks persisted due to the process's limits. The maximum SR improvement was 33.7, whereas the minimum SR improvement was 0.476. Due to the inconsistency in magnification between the pre-process and post-process images, an exact scale comparison could not be conducted. Consequently, an approximate scale was utilized solely for reference. Based on the actual sample size, which ranged from approximately 1.0 cm to 1.3 cm, and considering the applied magnification of 20×, the estimated field of view (FOV) in the captured images corresponds to approximately 500 µm to 650 µm in real-world dimensions. The MAF process is suitable for complex geometric designs and high-cost manufacturing, as it eradicates microcracks and achieves precise tolerances. Figure 13 depicts the changes in surface topology before and after the implementation of the MAF process on the samples. Table 8 highlights the surface enhancements achieved using the magnetic abrasive finishing (MAF) process. These include a decrease in surface roughness, ultra-smooth surfaces with Ra values below 0.1 µm, and enhanced surface uniformity. This study illustrates the effective elimination of micro-cracks from intricately curved turbine blades, enhancing surface roughness, prolonging component lifespan, and enabling timely rehabilitation before substantial damage. Optical microscopy was employed in this process to assess the surface topography, as it allows observation of a relatively large surface area compared to scanning electron microscopy (SEM), which typically provides highly localized or point-specific images. The researcher aimed to capture as much of the surface terrain as possible to evaluate the extent of crack removal achieved through the MAF (Magnetic Abrasive Finishing) process. Therefore, optical microscopy was selected as the preferred method, as it enables broader illumination and visualization of the treated metal surface. The scratches observed on samples 1, 2, 6, 8, and 9 after MAF are attributed to non-optimal process parameters—such as large working gaps, high abrasive ratios, and unstable brush flexibility. In these cases, the sharp Al_2O_3 particles may have acted abrasively in a non-uniform manner, causing surface scratches rather than smooth polishing. Additionally, fractured or poorly distributed abrasive particles may have contributed to these marks. This points out that it requires precise parameter control to ensure consistent and defect-free finishing.

Table 8: A comparison between the current work and the other works using the MAF process

Aim of the study	Description	MAF Process Type	Key Input Parameters	Workpiece	Ref.
Using different abrasive fine-finishing technologies to reduce (Ra)	Best Ra was achieved on ultra-smooth surfaces (Ra < 0.1 µm) at MAF.	Rotational MAF	- Magnetic flux: 0.5 T - Abrasive: SiC (5 µm) - RPM: 800 - Gap: 1.5 mm	T-15 Steel Stainless Steel (AISI 304)	[37]
Improved Surface Uniformity	Eliminates irregularities, creating a homogeneous surface.	Vibratory MAF	- Magnetic flux: 0.3 T - Abrasive: Diamond (3 µm) - Frequency: 50 Hz	Titanium Alloy (Ti-6Al-4V)	[38]
Removal of Micro-Cracks and Burrs	Polishes edges and removes subsurface defects.	Stationary MAF	- Magnetic flux: 0.7 T - Abrasive: Al_2O_3 (10 µm) - Feed rate: 5 mm/min	Tool Steel (D2)	[39]
Compressive Residual Stresses	Enhances fatigue life by inducing beneficial residual stresses.	Hybrid MAF (ECM + MAF)	- Magnetic flux: 0.6 T - Abrasive: B_4C (7 µm) - Current: 2 A (ECM)	Nickel-Based Superalloy (Inconel 718)	[40]
Enhanced Surface Hardness	Work-hardens the surface layer due to abrasive action.	Linear MAF	- Magnetic flux: 0.4 T - Abrasive: SiO_2 (15 µm) - Speed: 0.2 m/s	Aluminum Alloy (6061)	[41]
Improved Corrosion Resistance	Smoother surfaces reduce sites for corrosion initiation.	Ultrasonic-Assisted MAF	- Magnetic flux: 0.2 T - Abrasive: CeO_2 (8 µm) - Ultrasonic power: 200 W	Magnesium Alloy (AZ31B)	[42]
This Study: Crack Removal & SR Improvement	Removed fatigue cracks, improved SR by 33.7%, and extended life	MAF Rotational for flat surface	- Al_2O_3 (300 µm), 630 rpm, 1.8 mm gap, 30% mix	Compressor blades turbine AISI 403 stainless steel	This study

In Figure 13, the colored circles highlight micro-cracks and surface defects such as pits and protrusions present before the MAF process. These imperfections were effectively removed, and the surface was significantly improved after the application of MAF, as illustrated by the differences in surface topography before and after processing. However, in a few cases, no significant surface changes were observed after MAF. This may be attributed to variations in the operational conditions during the MAF process or to the fact that the surfaces did not exhibit notable cracks or surface deterioration during their service life. Variations in operational conditions during MAF can significantly impact surface improvement effectiveness. These include changes in tool rotation speed, working gap, abrasive mixing ratio, magnetic field strength, abrasive particle characteristics, and processing time. Overly high or low rotation speeds can reduce polishing efficiency, while improper working gaps can weaken the magnetic field. Inconsistencies in the iron-to-abrasive particle ratio can cause uneven material removal. Short processing times can result in inadequate surface modification.

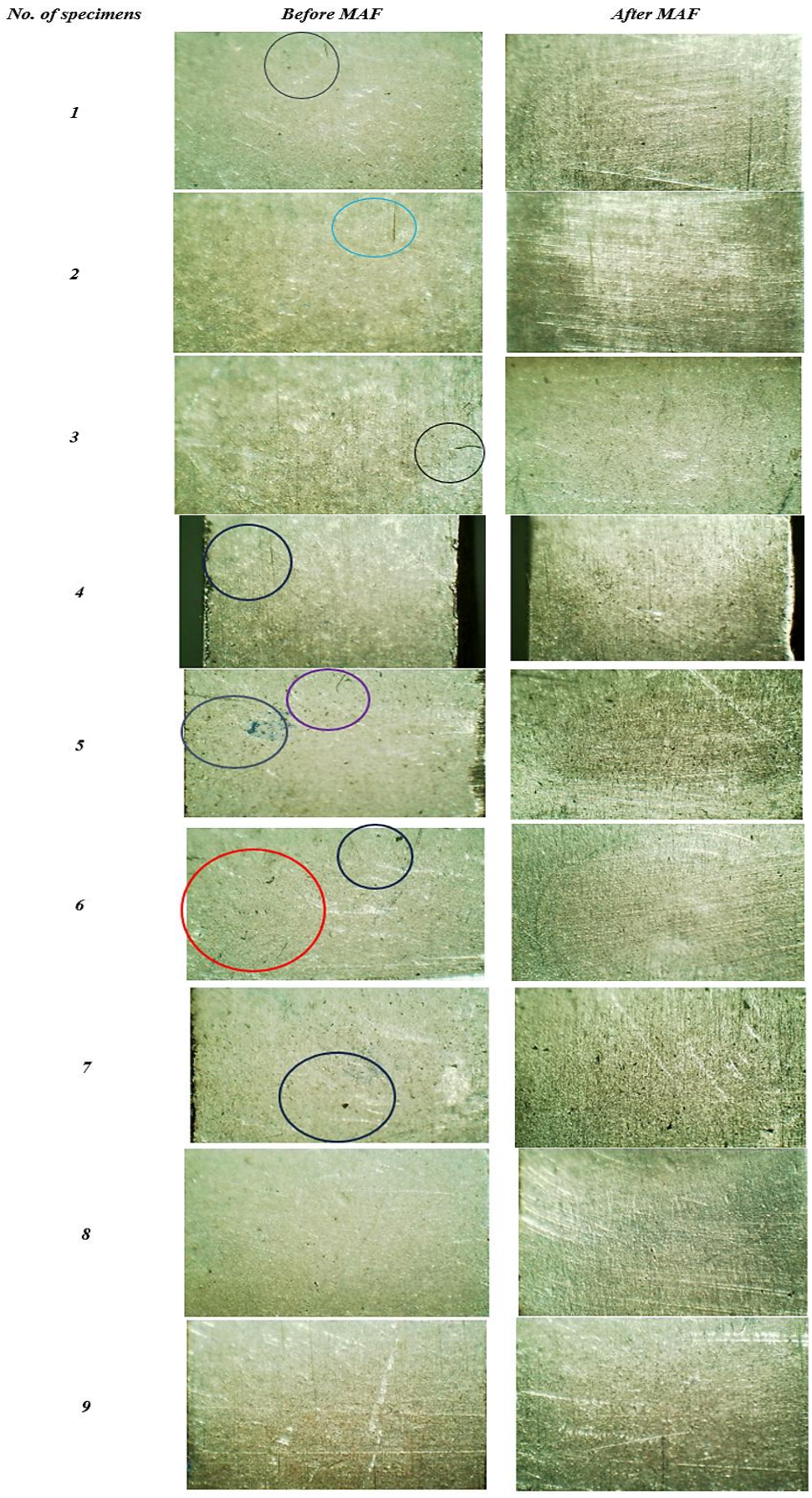

Figure 13: Surface topology comparison before and after MAF treatment

5. Discussions

The elimination of microcracks from metal surfaces provides strong evidence for the enhancement of product longevity, especially in components with intricate geometries subjected to heat gradients. Microcracks function as significant stress concentrators and can act as nucleation sites for bigger fractures under thermal or mechanical stress. In areas with complex shapes, stress builds up more at corners and changes in shape, so having microcracks greatly raises the chances of cracks spreading and causing failure. Moreover, temperature fluctuations induce uneven expansion and contraction of components, resulting in recurrent stress that exacerbates the development of surface imperfections. Eliminating microcracks enhances surface integrity, diminishes stress concentration spots, and postpones the emergence of fatigue damage. This advantage is particularly significant in automotive and aerospace applications, where components frequently endure elevated temperatures and mechanical stresses. Eliminating microcracks enhances components' resistance to wear and corrosion, hence prolonging their lifespan and ensuring more reliable performance under elevated temperatures and stress. This study offers a systematic assessment of magnetic abrasive finishing (MAF) employing aluminum oxide (Al_2O_3) as one of the powder compounds to improve the surface integrity of gas turbine compressor blades. The research specifically sought to eliminate fatigue-induced micro-cracks while preserving dimensional accuracy. Using the Taguchi L9 method, the effects of rotational speed, gap distance, and abrasive mixing ratio on surface roughness (SR) and material removal rate (MRR) were assessed.

5.1 Surface roughness (SR) improvement

The MAF process demonstrated significant potential in improving surface roughness. The most substantial enhancement in surface finish was achieved at: Rotation speed: 630 rpm, Gap distance: 1.8 mm, Mixing ratio: 30%, Surface roughness improvement (ΔSR): 33.7%.

Al_2O_3 abrasives achieved optimal surface finishing by smoothing micro-topographies and removing fatigue micro-cracks. In contrast, specimen #1 showed a 0.476% deterioration in surface roughness, likely caused by overly stiff abrasives and contamination from abrasive particle debris. Analysis of variance (ANOVA) for surface roughness (SR) revealed that rotation speed had the most statistically significant impact, with a P-value of 0.050. In contrast, the effects of gap distance and abrasive ratio were less pronounced, yielding P-values of 0.407 and 0.874, respectively. Also, checking the regression model showed that the leftover values were almost normally distributed, which supports that the model is reliable and accurate in predicting surface roughness outcomes.

5.2 Material removal rate (MRR)

MRR varied among the samples, with the highest rate achieved under, Speed: 400 rpm, Gap distance: 1.8 mm, Mixing ratio: 40%, MRR: 0.0195 g/min. This indicates that while elevated speeds (800 rpm) were anticipated to enhance MRR, they instead destabilized the magnetic abrasive brush, resulting in reduced efficacy. Excessive centrifugal force may result in the detachment of abrasive particles from the surface. Analysis of Variance for Material Removal Rate The model indicated that rotation speed, gap, and mixing ratio exhibited no statistically significant individual effects ($P > 0.05$); however, their combination significantly influenced the results.

5.3 Surface topography analysis

Microscopy indicated a significant decrease in surface irregularities following MAF. Micro-cracks, pits, and asperities were predominantly eliminated, particularly in samples treated under optimal conditions. Nonetheless, samples exhibiting significant abrasive gaps or inadequately mixed abrasives demonstrated minimal enhancements. This underscores the process's sensitivity to parameter regulation MAF resulted in: Reduction in Ra values below 0.1 μm, Micro-crack elimination, Polishing of complex geometries without deformation, Enhanced fatigue resistance due to the removal of micro-cracks and surface enhancement.

A visual comparison in Figure 11 further validated the removal of surface defects. Optical microscopy was preferred over SEM to capture a broader area and better assess surface uniformity. This study specifically addresses the elimination of fatigue-induced microcracks in gas turbine blades, a previously underexamined domain. This study prioritizes durability enhancement and the feasibility of local reconditioning, in contrast to other works that emphasize finishing or hardness.

5.4 Research significance and innovations

5.4.1 Novelty

In contrast to previous studies focused on polishing or surface uniformity, this research addresses the removal of fatigue crack layers—a significant concern in aerospace and energy sectors.

5.4.2 Innovation

Tailored MAF system employing a 5200-turn copper coil for regulated magnetic field generation.

5.4.3 Material Emphasis

Employment of AISI 403 stainless steel blades—prevalent in turbines yet challenging to finish due to their hardness and geometry.

5.4.4 Local Industry Impact

Exhibits the potential for domestic blade reconditioning, resulting in cost reductions of up to 50% compared to imports.

This comprehensive results section illustrates the efficacy, obstacles, and extensive applicability of the MAF process utilizing Al_2O_3 abrasives. In the end, the study shows that using Al_2O_3 abrasives in MAF is a good and promising way to improve the fatigue resistance and surface quality of turbine blades, as long as the process settings are adjusted to fit the specific material and shape of the parts.

Future research should look into creating mathematical models for batch processing, finding ways to reduce costs and improve efficiency, setting up standard quality control practices, and studying how abrasive particles behave in different working conditions.

6. Conclusions and future work

This study evaluated the effectiveness of Magnetic Abrasive Finishing (MAF) using alumina (Al_2O_3) abrasive powder for improving the surface integrity of gas turbine compressor blades. The experimental findings revealed substantial enhancements in surface finish and fatigue resistance, with the optimal performance achieved at a rotational speed of 630 rpm, a working gap of 1.8 mm, and an abrasive concentration of 30%. The MAF process consistently reduced surface roughness—achieving up to a 33.7% improvement—and effectively eliminated micro-scale surface defects and mitigated microcrack formation, thereby extending component service life. Additionally, the maximum material removal rate was observed under different conditions: a working gap of 1.8 mm, an abrasive concentration of 40%, and a rotational speed of 400 rpm. Despite these positive outcomes, the process exhibited certain limitations, notably in one experimental scenario where a 0.476% deterioration in surface finish was recorded. These limitations were primarily attributed to brush stiffness, the large size of abrasive particles, and the potential for surface contamination from fractured Al_2O_3 particles. Nevertheless, the process demonstrated particular effectiveness in applications involving complex geometries, high-precision manufacturing, and the removal of microcracks in critical components. Al_2O_3 abrasives maintained their effectiveness under moderate processing conditions and showed durability across most trials. However, challenges such as particle fracture at excessive working gaps and abrasive embedment in the workpiece surface were noted. Based on these observations, future research is recommended to focus on the development of mathematical models for batch processing, optimization of cost and efficiency, the implementation of standardized quality control measures, and a deeper investigation into abrasive particle behavior under various operating conditions. Ultimately, the study confirms that MAF employing Al_2O_3 abrasives is a viable and promising approach for enhancing the fatigue resistance and surface quality of turbine blades, provided that process parameters are carefully tailored to the specific material and geometrical characteristics of the components.

Acknowledgment

We extend our gratitude to the Department of Engineering and Metallurgy at the University of Technology in Baghdad, Iraq. I would like to thank Diyala General Company for helping me manufacture the MAF coil and run the samples. I would also like to thank Al-Quds Electric Power Plant for providing gas turbine blades.

Author contributions

Conceptualization, **T. Salman**, and **S. Shather**; data curation, **B. Albaghdadi**; formal analysis, **T. Salman**; investigation, **B. Albaghdadi**; methodology, **S. Shather**; project administration, **S. Shather**; resources, **T. Salman**; software, **B. Albaghdadi**; supervision, **S. Shather**; validation, **T. Salman**, **S. Shather**, and **B. Albaghdadi**; visualization, **B. Albaghdadi**; writing—original draft preparation, **T. Salman**; writing—review and editing, **S. Shather**, and **B. Albaghdadi**. All authors have read and agreed to the published version of the manuscript.

Funding

This research received no specific grant from any funding agency in the public, commercial, or not-for-profit sectors.

Data availability statement

The data that support the findings of this study are available on request from the corresponding author.

Conflicts of interest

The authors declare that there is no conflict of interest.

References

[1] P. Y. Wu, M. Hirtler, M. Bambach, and H. Yamaguchi, Effects of build-and scan-directions on magnetic field-assisted finishing of 316L stainless steel disks produced with selective laser melting, CIRP J. Manuf. Sci. Technol., 31 (2020) 583-594. https://doi.org/10.1016/j.cirpj.2020.08.010

[2] A. R. Mohammed and W. K. Jawad, Practical test and FEA to evaluation of the thickness distribution for octagonal cup generated by deep drawing, AIP Conference Proceedings, 3002 (2024) 080022. https://doi.org/10.1063/5.0205959

[3] J. Wu, Y. Zou, and H. Sugiyama, Study on ultra-precision magnetic abrasive finishing process using low-frequency alternating magnetic field, J. Magn. Magn. Mater., 386 (2015) 50-59. https://doi.org/10.1016/j.jmmm.2015.03.041

[4] K. Anjaneyulu and G. Venkatesh, Surface texture improvement of magnetic and nonmagnetic materials using the magnetic abrasive finishing process, Proc. Inst. Mech. Eng. C: J. Mech. Eng. Sci., 235 (2021) 4084-4096. https://doi.org/10.1177/0954406220970590

[5] B. Xing and Y. Zou, Investigation of finishing aluminum alloy A5052 using the magnetic abrasive finishing combined with electrolytic process, Machines, 8 (2020) 1-14. https://doi.org/10.3390/machines8040078

[6] P. Kala, V. Sharma, and P. M. Pandey, Surface roughness modelling for Double Disk Magnetic Abrasive Finishing process, J. Manuf. Process, 25 (2017) 37-48. https://doi.org/10.1016/j.jmapro.2016.10.007

[7] A. M. Ahmed, and S. K. Shather, Optimizing the five magnetic abrasive finishing factors on surface quality using Taguchi-based grey relational analysis, Eng. Res. Expr., 6 (2024) 015405. https://doi.org/10.1088/2631-8695/ad2d99

[8] J. Wu, Y. Zou, and H. Sugiyama, Study on finishing characteristics of magnetic abrasive finishing process using low-frequency alternating magnetic field, Int. J. Adv. Manuf. Technol., 85 (2016) 585-594. https://doi.org/10.1007/s00170-015-7962-9

[9] Y. Choopani, M. R. Razfar, P. Saraeian, and M. Farahnakian, Experimental investigation of external surface finishing of AISI 440C stainless steel cylinders using the magnetic abrasive finishing process, Int. J. Adv. Manuf. Technol., 83 (2016) 1811-1821. https://doi.org/10.1007/s00170-015-7700-3

[10] A. Singh, P. Singh, A. Kaushik, S. Singh, L. Singh, A. Singh, B. Ram, Comparative assessment of abrasives in magnetic abrasive finishing: An experimental performance evaluation, J. Magn. Magn. Mater., 604 (2024) 172312. https://doi.org/10.1016/j.jmmm.2024.172312

[11] V. V. Maksarov and A. I. Keksin, Technology of magnetic-abrasive finishing of geometrically-complex products, IOP Conf. Ser. Mater. Sci. Eng., 327 (2018) 042068. https://doi.org/10.1088/1757-899X/327/4/042068

[12] H. Xie, Y. Zou, Investigation on finishing characteristics of magnetic abrasive finishing process using an alternating magnetic field, Machines, 8 (2020) 1-17. https://doi.org/10.3390/machines8040075

[13] M. N. Houshi, A Comprehensive Review on Magnetic Abrasive Finishing Process, Adv. Eng. Forum., 18 (2016) 1–20. https://doi.org/10.4028/www.scientific.net/AEF.18.1

[14] F. Ahmadi, H. Beiramlou, and P. Yazdi, Effect of abrasive particle morphology along with other influencing parameters in magnetic abrasive finishing process, Mech. Ind., 22 (2021) 15. https://doi.org/10.1051/meca/2021013

[15] K. Zhou, Y. Chen, Z. W. Du, and F. L. Niu, Surface integrity of titanium part by ultrasonic magnetic abrasive finishing, Int. J. Adv. Manuf. Technol., 80 (2015) 997-1005. https://doi.org/10.1007/s00170-015-7028-z

[16] S. S. Khangura, L. S. Sran, A. K. Srivastava, and H. Singh, Investigations into the removal of edm recast layer with magnetic abrasive machining, Int. Manuf. Sci. Eng. Conf., 1 (2015) 1-6. https://doi.org/10.1115/MSEC2015-9259

[17] J. Zhang, A. Chaudhari, and H. Wang, Surface quality and material removal in magnetic abrasive finishing of selective laser melted 316L stainless steel, J. Manuf. Process., 45 (2019) 710-719. https://doi.org/10.1016/j.jmapro.2019.07.044

[18] K. Arora and A. K. Singh, Theoretical and experimental investigation on surface roughness of straight bevel gears using a novel magnetorheological finishing process, Wear, 476 (2021) 203693. https://doi.org/10.1016/j.wear.2021.203693

[19] S. Ahmad, R. M. Singari, and R. S. Mishra, Development of Al2O3-SiO2 based magnetic abrasive by sintering method and its performance on Ti-6Al-4V during magnetic abrasive finishing, Trans. Inst. Met. Finish., 99 (2021) 94-101. http://dx.doi.org/10.1080/00202967.2021.1865644

[20] Y. Wang, C. C. Tang, H. Y. Chai, Y. Z. Chen, R. Q. Jin, W. Xiong, Study on removal of recast layer of NiTi shape memory alloy machined with magnetic field-assisted WEDM-ECM complex process, Int. J. Adv. Manuf. Technol., 129 (2023) 4335-4354. https://doi.org/10.1007/s00170-023-12588-3

[21] Z. Li, J. Jia, S. Yang, Experimental study on polishing of fluid magnetic abrasives for the wire electrical discharge grinding surface of micro-shafts, Int. J. Adv. Manuf. Technol., 129 (2023) 2067-2085. https://doi.org/10.1007/s00170-023-12425-7

[22] S. A. Rasouli, D. Nori, Investigation of Mass Magnetic Abrasive Finishing Process on Compressor Blades, J. Modren Process. Manuf., 12 (2024) 5-26. https://doi.org/10.71762/mpmp.2023.996855

[23] G. C. Verma, P. Kala, and P. M. Pandey, Experimental investigations into internal magnetic abrasive finishing of pipes, Int. J. Adv. Manuf. Technol., 88 (2017) 1657-1668. https://doi.org/10.1007/s00170-016-8881-0

[24] V. Saxena, P. S. Yadav, H. S. Pali, Effect of magnetic abrasive machining process parameters on internal surface finish, Mater. Today Proc., 25 (2019) 842–847. https://doi.org/10.1016/j.matpr.2019.11.051

[25] A. Y. Jiao, H. J. Quan, Z. Z. Li, Y. Chen, Study of magnetic abrasive finishing in seal ring groove surface operations, Int. J. Adv. Manuf. Technol., 85 (2016) 1195-1205. https://doi.org/10.1007/s00170-015-8029-7

[26] R. A. Marín, J. A. Escobar, J. Lobo Guerrero, Failure Analysis of a Fighter Jet Engine Compressor Blade Due to Foreign Object Damage and High-Cycle Fatigue, J. Fail. Anal. Prev., 21 (2021) 1729-1738. https://doi.org/10.1007/s11668-021-01195-7

[27] R. Kumar and V. R. Komma, Recent advancements in magnetic abrasive finishing: a critical review, Eng. Res. Express, 6 (2024). https://doi.org/10.1088/2631-8695/ad2ef7

[28] B. Ayad , S. K. Shather, W. K. Hamdan, Improve the Micro-hardness of Single Point Incremental Forming Product Improve the Micro-hardness of Single Point Incremental Forming Product Using Magnetic Abrasive Finishing, Eng. Technol. J. 38 (2020) 1137-1142. https://doi.org/10.30684/etj.v38i8A.906

[29] S. K. Amineh, A. F. Tehrani, A. Mohammadi, Improving the surface quality in wire electrical discharge machined specimens by removing the recast layer using magnetic abrasive finishing method, Int. J. Adv. Manuf. Technol., 66 (2013) 1793–1803. https://doi.org/10.1007/s00170-012-4459-7

[30] A. Gottwalt-Baruth, P. Kubaschinski, M. Waltz, U. Tetzlaff, Influence of the cutting method on the fatigue life and crack initiation of non-oriented electrical steel sheets, Int. J. Fatigue., 180 (2024) 108073. https://doi.org/10.1016/j.ijfatigue.2023.108073

[31] K. B. Judal, V. Yadava, D. Pathak, Experimental Investigation of Vibration Assisted Cylindrical–Magnetic Abrasive Finishing of Aluminum Workpiece, Mater. Manuf. Processes, 28 (2013) 1196-1202. https://doi.org/10.1080/10426914.2013.811725

[32] Y. Zou, R. Satou, O. Yamazaki, H. Xie, Development of a new finishing process combining a fixed abrasive polishing with magnetic abrasive finishing process, Machines, 9 (2021) 1-14. https://doi.org/10.3390/machines9040081

[33] Y. Yang, Y. Xue, B. Li, Y. Fu, Y. Jiang, R. Chen, W. Hang, X. Sun, A Magnetic Abrasive Finishing Process with an Auxiliary Magnetic Machining Tool for the Internal Surface Finishing of a Thick-Walled Tube, Machines, 10 (2022). https://doi.org/10.3390/machines10070529

[34] HPL Machining. (n.d.). Understanding the magnetic abrasive finishing process in machining. HPL Machining Blog. https://hplmachining.com/blog/understanding-the-magnetic-abrasive-finishing-process-in-machining/

[35] L. Heng, J. S. Kim, J. H. Song, S. D. Mun, Application of Al2O3/iron-based composite abrasives on MAF process for inner surface finishing of oval-shaped tube: predicting results of MAF process using artificial neural network model, J. Mater. Res. Technol., 15 (2021) 3268-3282. https://doi.org/10.1016/j.jmrt.2021.09.146

[36] F. Hashimoto, H. Yamaguchi, P. Krajnik, K. Wegener, R. Chaudhari, H. W. Hoffmeister, Abrasive fine-finishing technology, CIRP Annals, 65 (2016) 597-620. https://doi.org/10.1016/j.cirp.2016.06.003

[37] C. Qian, Z. Fan, Y. Tian, Y. Liu, J. Han, J. Wang, A review on magnetic abrasive finishing, Int. J. Adv. Manuf. Technol., 112 (2021) 619–634. https://doi.org/10.1007/s00170-020-06363-x.

[38] D. K. Singh, H. S. Shan, Development of magneto-abrasive finishing process, Int. J. Mach. Tools Manuf., 42 (2002) 953-959. https://doi.org/10.1016/S0890-6955(02)00021-4

[39] H. Yamaguchi, T. Shinmura, R. Ikeda, Study of internal finishing of austenitic stainless steel capillary tubes by magnetic abrasive finishing, J. Manuf. Sci. Eng., 129 (2007). http://dx.doi.org/10.1115/1.2738957

[40] G. Z. Kremen, E. A. Elsayed, V. Rafalovich, Mechanism of material removal in magnetic abrasive finishing, Wear, 317 (2014) 153-161.

[41] P. Kala, P. M. Pandey, Comparison of finishing characteristics of two paramagnetic materials using MAF, Int. J. Adv. Manuf. Technol., 77 (2015) 997-1010.